

## Electronic supplementary information

### **Solvent-Mediated Engineering of Copper-Metalated Acetylenic Polymer Scaffolds for Enhanced Photoelectrochemical Performance**

*Tao Zhang<sup>a,b,\*</sup>, Shunqi Xu<sup>a,†</sup>, Yang Hou<sup>c,‡</sup>, Guoliang Chai<sup>d,‡</sup>, Davide Olianas<sup>e</sup>, Zhongquan Liao<sup>f</sup>, Alberto Milani<sup>e</sup>, Hanjun Sun<sup>a</sup>, Wei Li<sup>a</sup>, Zhe Zhang<sup>g</sup>, Stefan Mannsfeld<sup>g</sup>, Ehrenfried Zschech<sup>f</sup>, Matteo Tommasini<sup>e</sup> and Xinliang Feng<sup>a,\*</sup>*

---

## Methods

### Materials

All the reagents were obtained from Sigma-Aldrich and used as received. Copper wafer (MicroChemicals GmbH, Germany): Prime CZ-Si wafer 4 inch, one side polished, p-type (boron), total-thickness-variation < 10  $\mu\text{m}$ , 1-10  $\Omega\text{ cm}$ ; 10 nm titanium adhesion layer; 200 nm copper (purity > 99.9 %), root-mean-square roughness < 10 nm. Copper foil (thickness 0.25 mm, 99.98%) was purchased from Sigma-Aldrich. The monomers 2,5-diethynylthieno[3,2-b]thiophene and 1,3,5-trifluoro-2,4,6-triethynylbenzene are synthesized according to literatures<sup>1,2</sup>. The copper was consecutively washed with portions of 3 M HCl (in methanol), methanol and ethanol under ultrasonication (2 min), and dried under a flow of argon. The cleaned copper wafer was immediately used for catalysis.

### Synthesis of Cu-PTEB on Cu wafer or foil

Typically, TEB (5 mg, 0.033 mmol) and piperidine (10  $\mu\text{L}$ , 0.1 mmol) were added in a glass bottle containing 10 mL dichloromethane as solvent. The freshly cleaned copper was submerged into a reaction mixture and the polymerization starts immediately at room temperature on the Cu surface, which can be observed by the color change of the Cu surface. After reaction, the sample was immediately washed with fresh dichloromethane, methanol, and ethanol sequentially. Finally, the sample was blow-dried by a jet of dry nitrogen and a golden yellow film was obtained uniformly on the substrate.

### Transfer of Cu-PTEB film

To transfer the Cu-PTEB film (area: 1 $\times$ 2  $\text{cm}^2$ ; thickness: ca. 80 nm) from copper to other substrates, the film was coated with PMMA resist (Allresist GmbH product number AR-P671.04, dissolved in chlorobenzene), and cured at 90  $^{\circ}\text{C}$  for 10 min. The copper substrate was etched away by a water solution of ammonium persulfate (0.25  $\text{g mL}^{-1}$ ) in 2 h. After being rinsed thoroughly with deionized water, the PMMA/Cu-PTEB film was transferred to a target substrate (e.g. Ti plate, 1 $\times$ 3  $\text{cm}^2$ ). The samples were naturally dried in air for 1 h and stored in high vacuum (room temperature) for 24 h to enhance the adhesion of Cu-PTEB with targeted substrate surface. PMMA was removed by thorough rinsing in acetone and isopropyl alcohol.

---

### Synthesis of Cu-PTEB on other substrates

A planar substrate (e.g., SiO<sub>2</sub> wafer, graphite, titanium, glass, etc.) piece cleaned by water and ethanol was sandwiched with a copper wafer in a distance of  $d = 0.1$  mm adjusted by two spacers. The assembly was immersed in the reaction mixture as indicated above and the washing procedures are similar.

### PEC measurements

The PEC performance of the copper-metalated acetylenic polymer (Cu-PTEB, Cu-PDET, Cu-PDEB, or Cu-PTFTEB) based photocathodes were tested using a three-electrode setup containing working electrode, counter electrode (Pt wire), and reference electrode (Ag/AgCl). The simulated sunlight was from a 200 W Xenon lamp ( $100 \text{ mW cm}^{-2}$ ) coupled with an AM 1.5 G filter (Newport). An electrochemical analyzer (CHI 760E) was applied to measure the polarization characteristic of the electrodes, with a scan rate of  $1 \text{ mV s}^{-1}$ , and there is no correction on data for any losses of uncompensated resistance. The electrolyte (0.01 M Na<sub>2</sub>SO<sub>4</sub>, pH = 6.8) was degassed for 30 min by flushing high purity argon at room temperature (ca. 25 °C) before electrochemical measurement. The EIS spectra were recorded by applying a 10 mV AC signal in the frequency range from 100 K to 0.01 Hz at a DC bias of 0.3 V (i.e. -0.3 V vs. Ag/AgCl). Current density was calculated using exposed geometric surface area of  $1.0 \text{ cm}^2$  of the photoelectrode ( $J_{\text{photocurrent density}} = J_{\text{measured photocurrent}} / S_{\text{exposed geometric surface area}}$ ). The applied potential vs. Ag/AgCl is converted to RHE potential using the following equation:  $E_{\text{RHE}} = E_{\text{Ag/AgCl}} + 0.059 \text{ pH} + E_{\text{Ag/AgCl}}^0$  ( $E_{\text{Ag/AgCl}}^0 = 0.199 \text{ V}$ ).

### DFT calculations of Raman spectra

DFT calculations were carried out with the B3LYP functional using the Gaussian 09 software.<sup>3</sup> We adopted the 6-31+G (d,p) basis set to describe C and H atoms. The Cu atoms were described with the ECP10MDF Stuttgart pseudopotential and related VDZ basis set.<sup>4,5</sup> The model reported in Fig. S3 and Table S1 was obtained as a singlet state with total charge +1; the geometry was optimized under the constraint of C<sub>2v</sub> point group symmetry, which is representative of the local symmetry of the acetylenic-copper bridges expected in Cu-PTEB films (Fig. 1c). The calculations of the Raman activity were carried out after geometry optimization of such model.

### DFT calculations of HER processes

All the DFT calculations were performed by employing Quantum ESPRESSO code<sup>6</sup>. The generalized gradient approximation of Perdew-Burke-Ernzerhof (GGA-PBE) was adopted<sup>7</sup>, and spin polarization was considered for all the simulations. The kinetic energy cutoffs for the wavefunction and the charge were set to 45 Ry and 450 Ry, respectively. The free energy variation for each elementary step was calculated according to the method developed by Nørskov et al.<sup>8</sup> The total energies of intermediates are calculated and converted to free energies

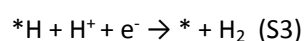
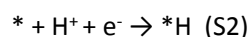
---

by adding zero-point energy, entropy, and solvation energy:

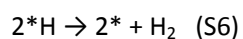
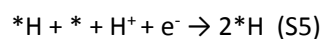
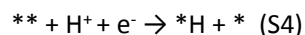
$$\Delta G = \Delta E_{\text{Total}} + \Delta E_{\text{ZEP}} - T\Delta S + \Delta G_s + 0.0591 * pH + eU \quad (S1)$$

where  $E_{\text{Total}}$  is the calculated total energy,  $\Delta E_{\text{ZPE}}$  is zero-point energy,  $\Delta S$  is entropy (0.37 eV), and  $\Delta G_s$  (-0.11 eV) is solvation energy for \*H intermediate.<sup>9,10</sup> The  $pH$  effect and potential effect were considered as  $0.0591 * pH$  and  $eU$ , respectively. Here, we take  $pH=0$  and  $U=0$  to calculate the free energy variation for each elementary step.

Both single site (Volmer-Heyrovsky) and dual sites (Volmer-Tafel) reaction pathways were considered for HER. The elementary steps for single site HER process are:



Where \* denotes catalytic site. For dual sites HER, the elementary steps are:



There are five possible different catalytic sites in Cu-PTEB as shown in Fig. S15 in the main text. The reaction free energies for elementary steps were calculated for all the different sites via both single and dual sites processes. The results are presented in Fig. S16 and Fig. S17, respectively. We can see from the results that the site 5 is the most favorable site for single site HER and the 45 sites are the most favorable sites for dual sites HER.

### Other characterizations

The morphology of Cu-PTEB were characterized using a field emission scanning electron microscope (FESEM) (Carl Zeiss Gemini 500) equipped with an energy-dispersive X-ray (EDX) spectrometer. Transmission electron microscopy (TEM) images were obtained using a Cs corrected TEM (Carl Zeiss Libra 200) operated at 200 kV. For TEM studies, the samples were grown directly on a copper grid. TEM image of the Cu-PTEB were taken on the edge of the grid. Optical images were acquired in differential interference mode using an optical microscope (Carl Zeiss AxioScope A1).

Raman spectra were acquired on confocal Raman microscope (NT-MDT) using a 532 nm (2.33 eV) laser. A background-correction was performed on the Raman data in Figs. 1b and 1d for a better comparison with simulated result. Fourier transform infrared spectra (FTIR) were collected with a BRUKER TENSOR II spectrometer.

X-ray photoelectron spectroscopy (XPS) and UV photoelectron spectroscopy (UPS) were

---

performed in ultra-high vacuum (base pressure  $10^{-10}$  mbar) with an ESCALAB™ 250Xi XPS Microprobe (Thermo Scientific™), using Al K $\alpha$  X-Ray source ( $h\nu = 1486.6$  eV, monochromatized) and HeI discharge lamp for excitation, respectively. Pass energy was 200 eV for survey XPS spectrum, 20 eV for high-resolution C1s spectrum, and 3 eV for the UPS spectrum.

UV-vis spectroscopy was performed on NR 5000 (Agilent technologies, 172 Germany) using the Cu-PTEB film grown on quartz glass in transmission mode.

$I$ - $V$  curves of Cu-PTEB was measured using a semiconductor analyzer (Keithley 4200) at 25 °C and relative humidity (RH) = 20%. Data were collected over a voltage range of -30 to 30 V using the linear sweep mode. The devices were prepared by transferring Cu-PTEB film on commercial OFET substrates (Fraunhofer IPMS, Dresden).

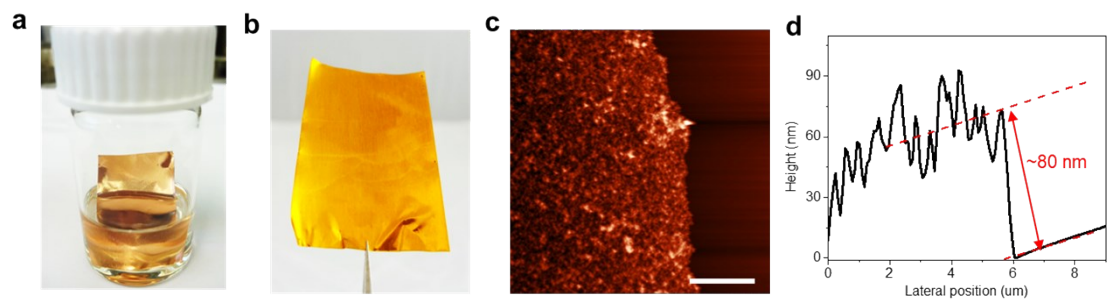


**Figure S1.** (a) Photography of the reaction mixture in the synthesis of Cu-PTEB. (b) As prepared Cu-PTEB on Cu foil. (c) AFM topographic image of PTEB on SiO<sub>2</sub>/Si wafer, scale bar, 5 μm. (d) Height profile selected in (c).

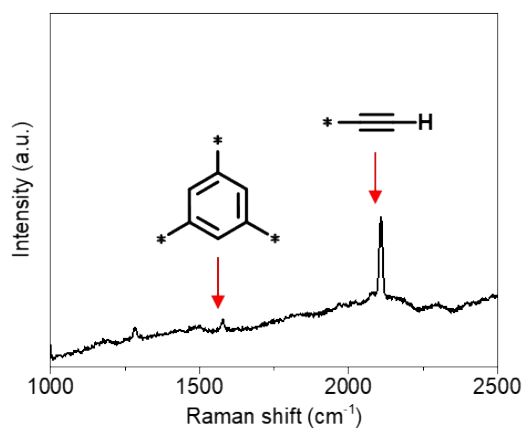


**Figure S2. Raman spectrum and peak assignment of TEB monomer.**

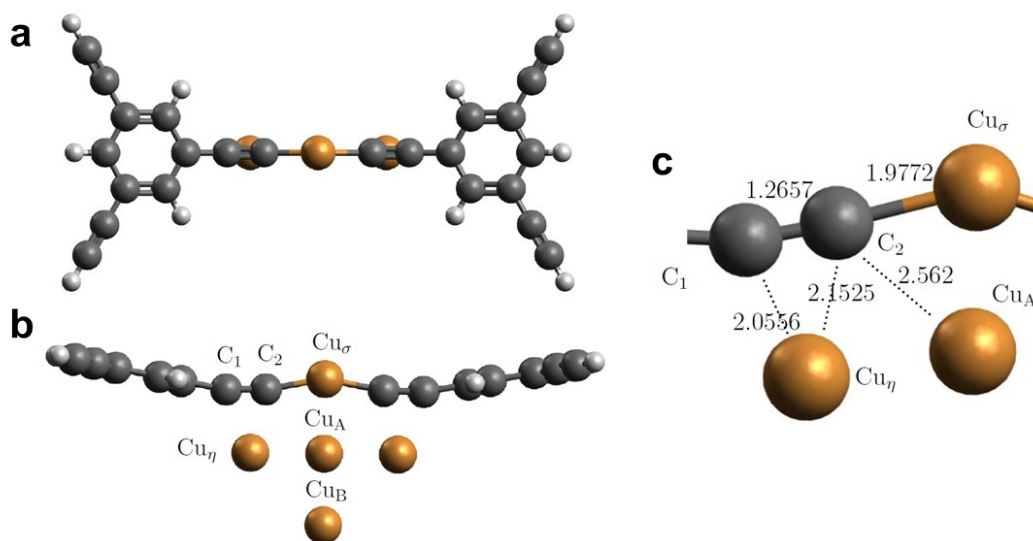


**Figure S3.** (a) Top view and (b) side view of the calculated Cu-PTEB model ( $C_{2v}$  point group symmetry; singlet state, total charge +1). (c) Bond lengths of the model, which show  $\eta^2$ -coordination of the  $C\equiv C$  bond with copper; accordingly, NBO analysis reveals an overall decrease of 0.15 electronic charges in the 3d orbitals of  $Cu_\eta$ .

---

**Table S1. Peak assignments for the Cu-PTEB model.**

---

Main computed Raman peaks (cm <sup>-1</sup> , frequency scaled by 0.98)	Mode description
2176	terminal C≡C stretching
1929	Cu-coordinated C≡C stretching
1576	ring stretching
1286	ring deformation
1138	C-C stretching, in-plane CH bending
986	ring deformation

---

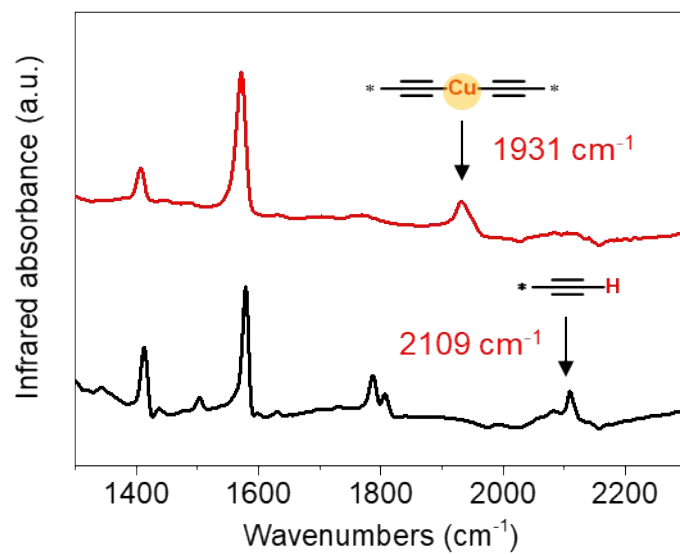


Figure S4. FTIR spectra and peak assignments of Cu-PTEB (red line) and monomer TEB (black line).

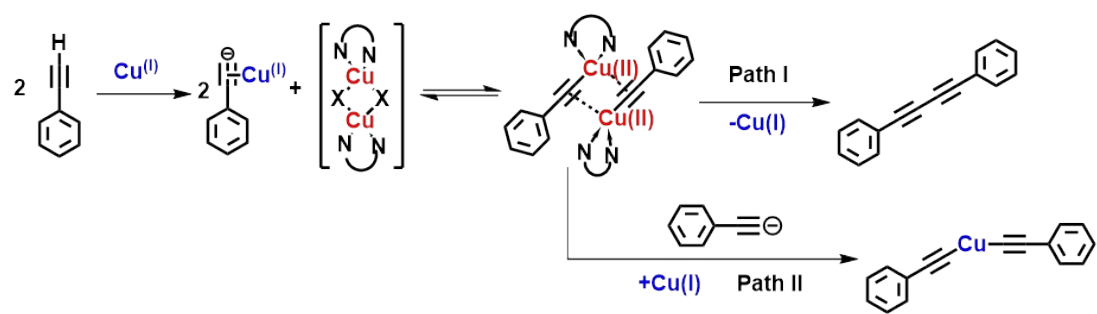
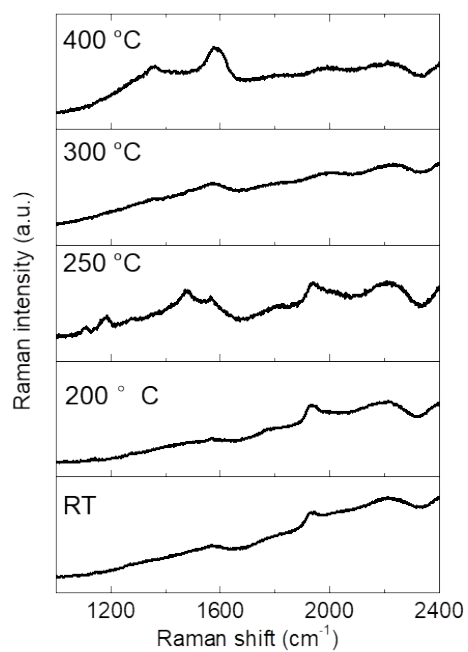
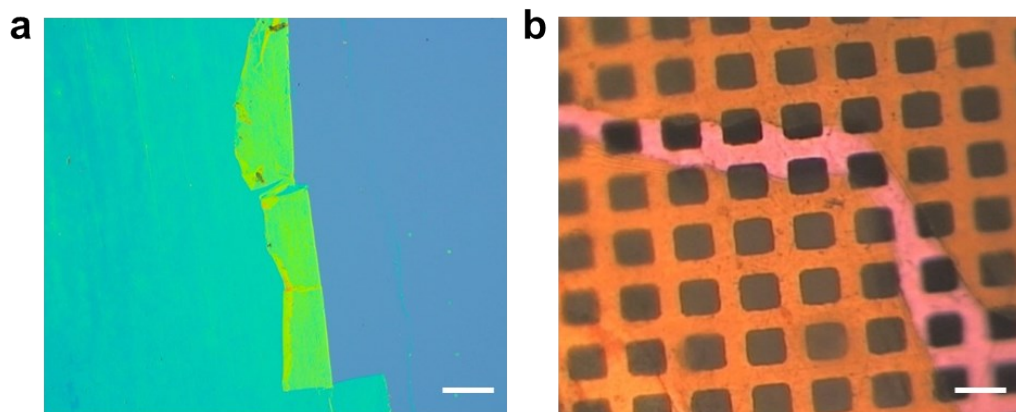


Figure S5. Proposed mechanism for the formation of Cu-PTEB structure.



**Figure S6. Raman spectra of Cu-PTEB annealed at different temperatures in argon atmosphere.**



**Figure S7. Optical microscopic images of Cu-PTEB.** (a) Cu-PTEB film transferred onto SiO<sub>2</sub>/Si; (b) free-standing Cu-PTEB film on Cu grid. Scale bars: 20 μm.

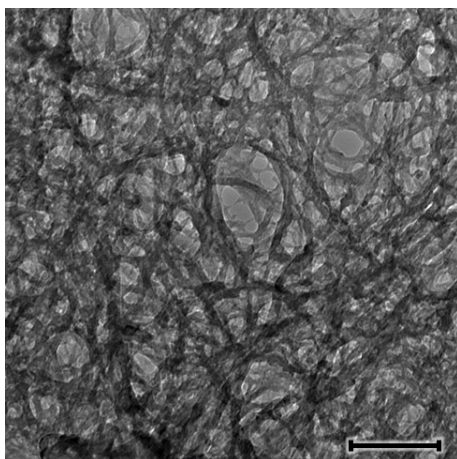


**Figure S8.** Transmission electron microscopy (TEM) image of Cu-PTEB on Cu grid. Scale bar: 200 nm.

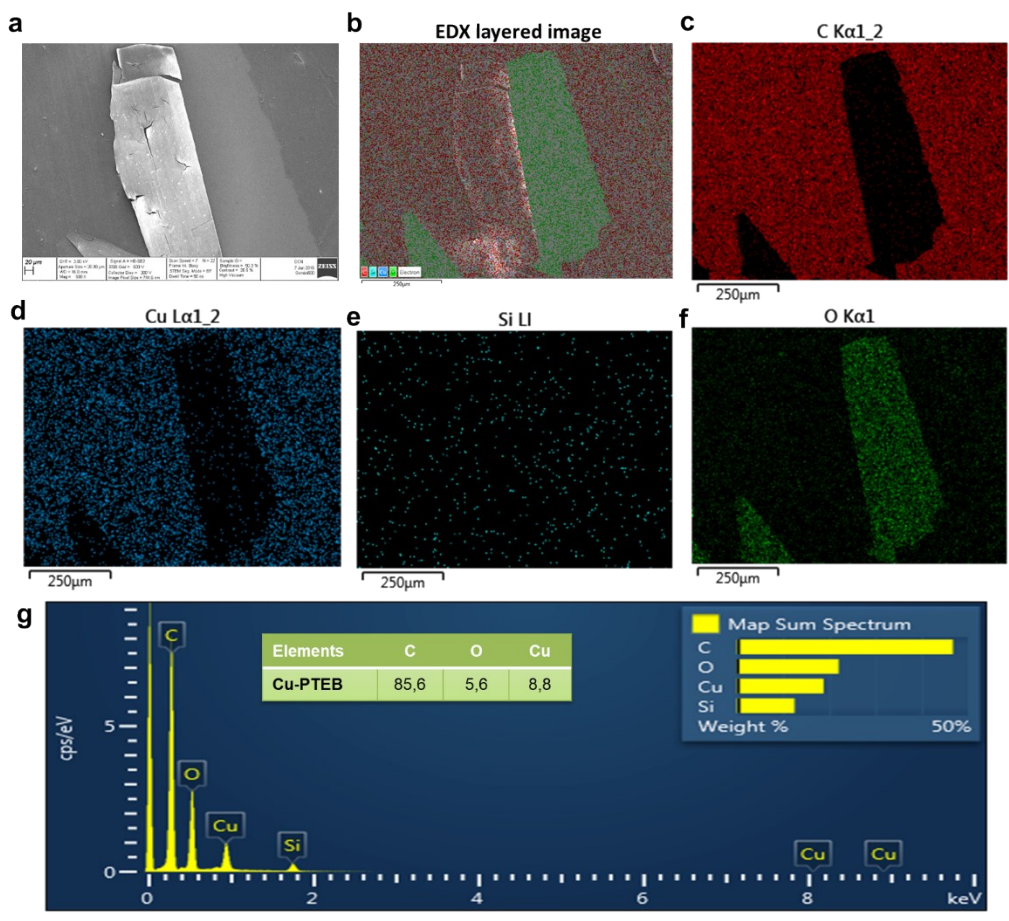


**Figure S9.** SEM image and energy dispersive X-ray (EDX) elemental mapping images of Cu-PTEB transferred on SiO<sub>2</sub>/Si wafer. (a) SEM image of sample surface. Further EDX maps show clear contrast of different elements on the sample: (b) full elemental map, (c) carbon, (d) copper, (e) silicon and (f) oxygen. (g) The EDX spectrum corresponding to (b) was measured at 3 kV acceleration voltage.

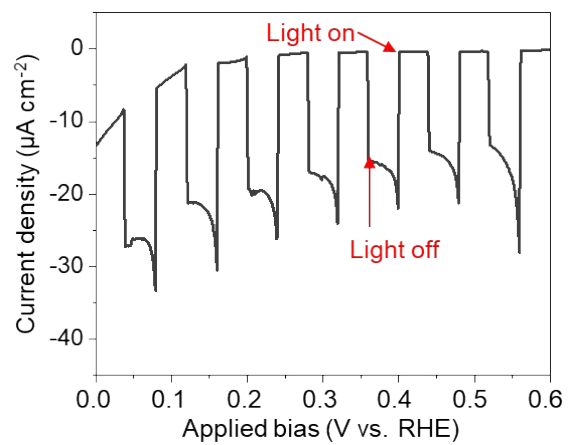
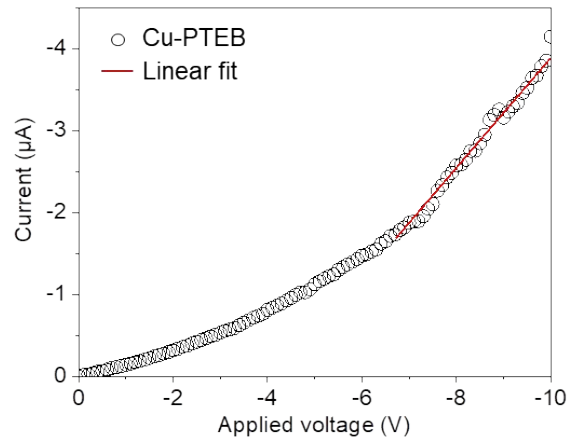
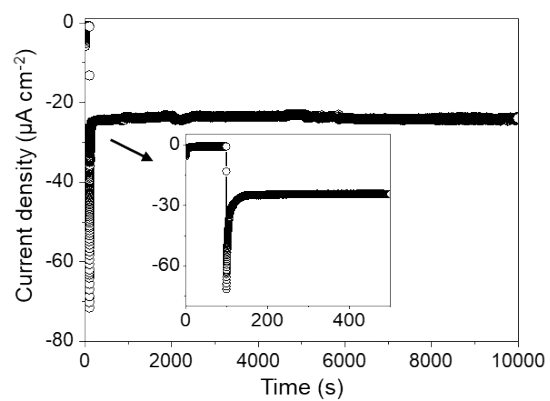


Figure S10. Current density curve vs. applied bias of Cu-PTEB under intermittent light irradiation.



**Figure S11. Electric conductivity of the Cu-PTEB film.** Representative  $I$ - $V$  characteristic curves of Cu-PTEB on the  $2.5\ \mu\text{m}$  channel OFET device, which exhibits semiconductor-like characteristics<sup>15</sup>. The average thickness of the polymer films is *ca.* 180 nm.  $R$  of the sample was estimated from the inverse slope of the  $I$ - $V$  curve. When the  $I$ - $V$  curve is not linear, the slope of the curve was estimated from the linear fit of the curve. Thus, the conductivity,  $\sigma$ , of the Cu-PTEB film was found to be of *ca.*  $8.7 \times 10^{-5}$  S/cm, which is about 30 times greater than PTEB film (*i.e.*  $3.0 \times 10^{-6}$  S/cm).



**Figure S12.** Current density vs. time of PTEB photocathode under illumination for 10000 s. The test was performed at 0.3 V vs. RHE under AM 1.5G irradiation.

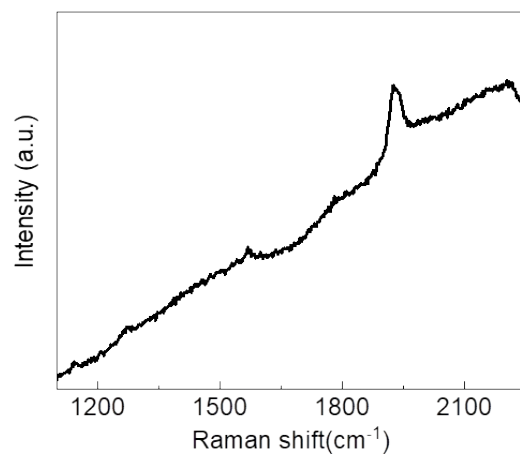


**Figure S13. Raman spectrum of Cu-PTEB photocathode after PEC HER test.**

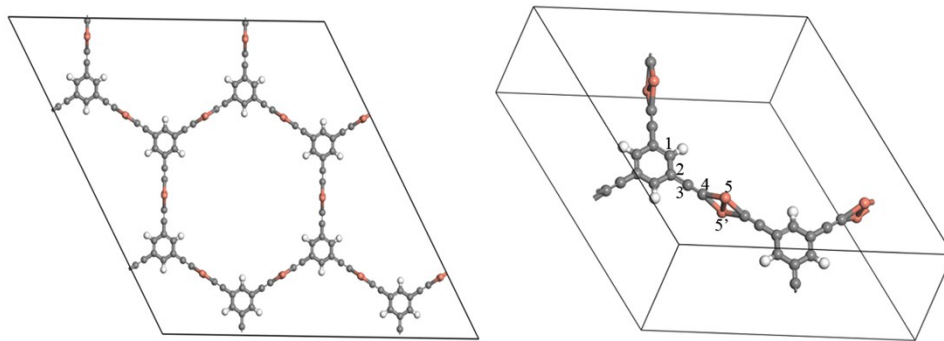


**Figure S14. Atomic structure of simulation supercell (left) and unit cell (right) for Cu-PTEB.** The possible active sites are labelled as 1, 2, 3, 4, 5 and 5'. The carbon, hydrogen and copper atoms denoted as grey, white, and brown balls.

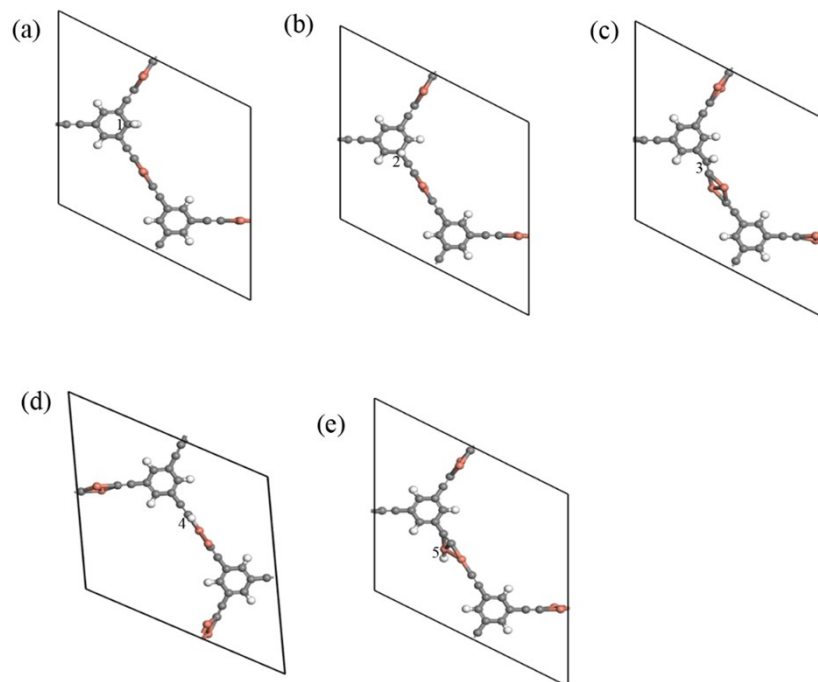


**Figure S15. Atomic structures of \*H at different sites of Cu-PTEB.** The carbon, hydrogen and copper atoms denoted as grey, white, and brown balls.

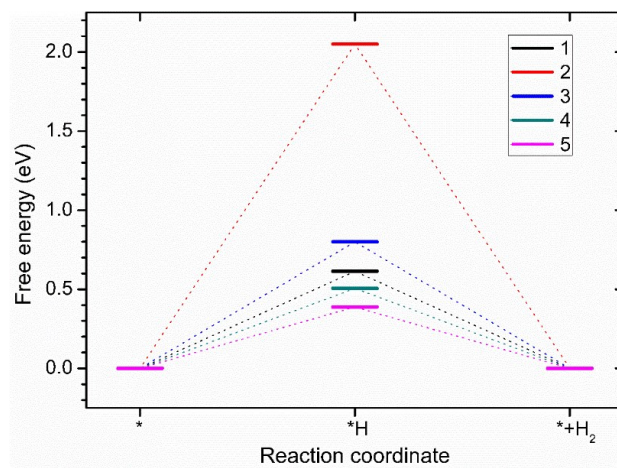


**Figure S16. Free-energy variations for HER via single site reaction pathway: 1, 2, 3, 4, 5, and 5' denote for different active sites as labeled in Fig. S14.**

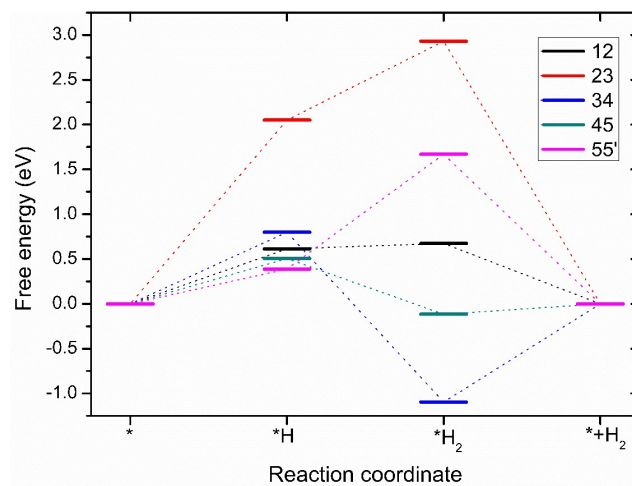


**Figure S17. Free energy variations for HER via dual sites reaction pathway.** 12, 23, 34, 45 and 55' denote for different active sites as labeled in main text.

**Table S2. Reported photocurrent densities of PEC photocathodes from COFs, MOFs and coordination polymers.**

Photocathode	Photocurrent density (J)	Potential*	Electrolyte	Light source
<i>g</i> -C <sub>3</sub> N <sub>4</sub> ( <i>Angew. Chem. Int. Edit.</i> 2016, 55, 14693)	0.3 μA cm <sup>-2</sup>	-1.0 V vs. Ag/AgCl	0.5 M Na <sub>2</sub> SO <sub>4</sub>	300 W Xenon lamp, λ > 420 nm
<i>g</i> -C <sub>3</sub> N <sub>4</sub> @C ( <i>Angew. Chem. Int. Edit.</i> 2016, 55, 10849)	0.7 μA cm <sup>-2</sup>	-0.1 V vs. Ag/AgCl	0.2 M Na <sub>2</sub> SO <sub>4</sub>	Keithley 6300 semiconductor analyzer
<i>g</i> -C <sub>x</sub> N <sub>y</sub> -COFs ( <i>Nat. Commun.</i> 2019, 10, 2467)	2.5 μA cm <sup>-2</sup>	-0.6 V vs. Ag/AgCl (i.e., 0 V vs. RHE)	0.2 M Na <sub>2</sub> SO <sub>4</sub>	300 W Xenon light with cut-off filter λ > 420 nm
BDT-ETTA COF ( <i>J. Am. Chem. Soc.</i> 2018, 140, 2085)	4.3 μA cm <sup>-2</sup>	-0.3 V vs. Ag/AgCl (i.e., 0.3 V vs. RHE)	0.1 M Na <sub>2</sub> SO <sub>4</sub>	AM1.5 solar simulator, 100 mW cm <sup>-2</sup>
A-TEXPY-COFs ( <i>Adv. Energy Mater.</i> 2018, 8, 1703278)	6 μA cm <sup>-2</sup>	-0.2 V vs. Ag/AgCl	1 M H <sub>2</sub> SO <sub>4</sub>	AM1.5 solar simulator, 100 mW cm <sup>-2</sup>
Poly-CuDMcT ( <i>ChemElectroChem</i> 2018, 5, 3847)	24 μA cm <sup>-2</sup>	-0.6 V vs. Ag/AgCl	0.5 M Na <sub>2</sub> SO <sub>4</sub>	400 W Xenon lamp
Cu <sub>3</sub> (BTC) <sub>2</sub> MOF@Cu <sub>2</sub> O ( <i>J. Am. Chem. Soc.</i> 2019, 141, 10924)	46 μA cm <sup>-2</sup>	-0.76 V vs. Ag/AgCl	0.01 M Na <sub>2</sub> SO <sub>4</sub>	300 W Xenon lamp, 64 mW cm <sup>-2</sup>
PTEB ( <i>Nat. Commun.</i> 2018, 9, 1140)	10 μA cm <sup>-2</sup>	-0.3 V vs. Ag/AgCl (i.e., 0.3 V vs. RHE)	0.01 M Na <sub>2</sub> SO <sub>4</sub>	200 W Xenon lamp (100 mW cm <sup>-2</sup> ), AM 1.5G filter
PTEB-co-PDET ( <i>Nat. Commun.</i> 2018, 9, 1140)	21 μA cm <sup>-2</sup>	-0.6 V vs. Ag/AgCl (i.e., 0 V vs. RHE)	0.01 M Na <sub>2</sub> SO <sub>4</sub>	200 W Xenon lamp (100 mW cm <sup>-2</sup> ), AM 1.5G filter
Cu-PTEB, <b>This work</b>	<b>22 μA cm<sup>-2</sup></b>	-0.3 V vs. Ag/AgCl (i.e., 0.3 V vs. RHE)	0.01 M Na <sub>2</sub> SO <sub>4</sub>	200 W Xenon lamp (100 mW cm <sup>-2</sup> ), AM 1.5G filter
Cu-PDET, <b>This work</b>	<b>70 μA cm<sup>-2</sup></b>	-0.3 V vs. Ag/AgCl (i.e., 0.3 V vs. RHE)	0.01 M Na <sub>2</sub> SO <sub>4</sub>	300 W Xe lamp, filter > 420 nm,
Cu-PDEB, <b>This work</b>	<b>38 μA cm<sup>-2</sup></b>	-0.3 V vs. Ag/AgCl (i.e., 0.3 V vs. RHE)	0.01 M Na <sub>2</sub> SO <sub>4</sub>	200 W Xenon lamp (100 mW cm <sup>-2</sup> ), AM 1.5G filter
Cu-PTFTEB, <b>This work</b>	<b>7 μA cm<sup>-2</sup></b>	-0.3 V vs. Ag/AgCl (i.e., 0.3 V vs. RHE)	0.01 M Na <sub>2</sub> SO <sub>4</sub>	200 W Xenon lamp (100 mW cm <sup>-2</sup> ), AM 1.5G filter

\* The follow equation was used to convert the potential vs. Ag/AgCl to RHE potential:  $E_{\text{RHE}} = E_{\text{Ag/AgCl}} + 0.059 \text{ pH} +$

$E_{\text{Ag/AgCl}}^0$  ( $E_{\text{Ag/AgCl}}^0 = 0.199 \text{ V}$ ; the potential vs. SCE to RHE potential:  $E_{\text{RHE}} = E_{\text{SCE}} + 0.059 \text{ pH} + E_{\text{SCE}}^0$  ( $E_{\text{SCE}}^0 = 0.242 \text{ V}$ ).

---

**Reference:**

- 1 Li, P.; Ahrens, B.; Feeder, N.; Raithby, P. R.; Teat, S. J.; Khan, M. S. *Dalton T.* **2005**, (5), 874-883.
- 2 Hennrich, G.; Echavarren, A. M. *Tetrahedron Lett.* **2004**, 45 (6), 1147-1149.
- 3 Gaussian 09, Revision D.01, M. J. Frisch, G. W. Trucks, H. B. Schlegel, G. E. Scuseria, M. A. Robb, J. R. Cheeseman, G. Scalmani, V. Barone, G. A. Petersson, H. Nakatsuji, X. Li, M. Caricato, A. Marenich, J. Bloino, B. G. Janesko, R. Gomperts, B. Mennucci, H. P. Hratchian, J. V. Ortiz, A. F. Izmaylov, J. L. Sonnenberg, D. Williams-Young, F. Ding, F. Lipparini, F. Egidi, J. Goings, B. Peng, A. Petrone, T. Henderson, D. Ranasinghe, V. G. Zakrzewski, J. Gao, N. Rega, G. Zheng, W. Liang, M. Hada, M. Ehara, K. Toyota, R. Fukuda, J. Hasegawa, M. Ishida, T. Nakajima, Y. Honda, O. Kitao, H. Nakai, T. Vreven, K. Throssell, J. A. Montgomery, Jr., J. E. Peralta, F. Ogliaro, M. Bearpark, J. J. Heyd, E. Brothers, K. N. Kudin, V. N. Staroverov, T. Keith, R. Kobayashi, J. Normand, K. Raghavachari, A. Rendell, J. C. Burant, S. S. Iyengar, J. Tomasi, M. Cossi, J. M. Millam, M. Klene, C. Adamo, R. Cammi, J. W. Ochterski, R. L. Martin, K. Morokuma, O. Farkas, J. B. Foresman, and D. J. Fox, Gaussian, Inc., Wallingford CT, **2016**.
- 4 Esboui, M.; Nsangou, M.; Jaidane, N.; Ben Lakhdar, Z. *Chem. Phys.* **2005**, 311 (3), 277-285.
- 5 Peterson, K. A.; Puzzarini, C. *Theor. Chem. Acc.* **2005**, 114 (4-5), 283-296.
- 6 Giannozzi, P.; Baroni, S.; Bonini, N.; Calandra, M.; Car, R.; Cavazzoni, C.; Ceresoli, D.; Chiarotti, G. L.; Cococcioni, M.; Dabo, I.; Dal Corso, A.; de Gironcoli, S.; Fabris, S.; Fratesi, G.; Gebauer, R.; Gerstmann, U.; Gougoussis, C.; Kokalj, A.; Lazzeri, M.; Martin-Samos, L.; Marzari, N.; Mauri, F.; Mazzarello, R.; Paolini, S.; Pasquarello, A.; Paulatto, L.; Sbraccia, C.; Scandolo, S.; Sclauzero, G.; Seitsonen, A. P.; Smogunov, A.; Umari, P.; Wentzcovitch, R. *M. J. Phys.-Condens. Mat.* **2009**, 21 (39).
- 7 Perdew, J. P.; Burke, K.; Ernzerhof, M. *Phys. Rev. Lett.* **1996**, 77 (18), 3865-3868.
- 8 Norskov, J. K.; Rossmeisl, J.; Logadottir, A.; Lindqvist, L.; Kitchin, J. R.; Bligaard, T.; Jonsson, H. *J. Phys. Chem. B* **2004**, 108 (46), 17886-17892.
- 9 Chai, G. L.; Boero, M.; Hou, Z. F.; Terakura, K.; Cheng, W. D. *ACS Catal.* **2017**, 7 (11), 7908-7916.

---

10 Chai, G. L.; Hou, Z. F.; Shu, D. J.; Ikeda, T.; Terakura, K. *J. Am. Chem. Soc.* **2014**, *136* (39), 13629-13640.